Supplementary Information:

Atomic coordination dictates vibrational characteristics and thermal conductivity in amorphous carbon

Ashutosh Giri,[1, a)] Connor Jaymes Dionne,[1] and Patrick E. Hopkins[2, 3, 4, b)]

[1)]*Department of Mechanical, Industrial and Systems Engineering, University of Rhode Island, Kingston, RI 02881, USA*

[2)]*Department of Mechanical and Aerospace Engineering, University of Virginia, Charlottesville, Virginia 22904, USA*

[3)]*Department of Materials Science and Engineering, University of Virginia, Charlottesville, Virginia 22904, USA*

[4)]*Department of Physics, University of Virginia, Charlottesville, Virginia 22904, USA*

[a)]Electronic mail: ashgiri@uri.edu

[b)]Electronic mail: phopkins@virginia.edu

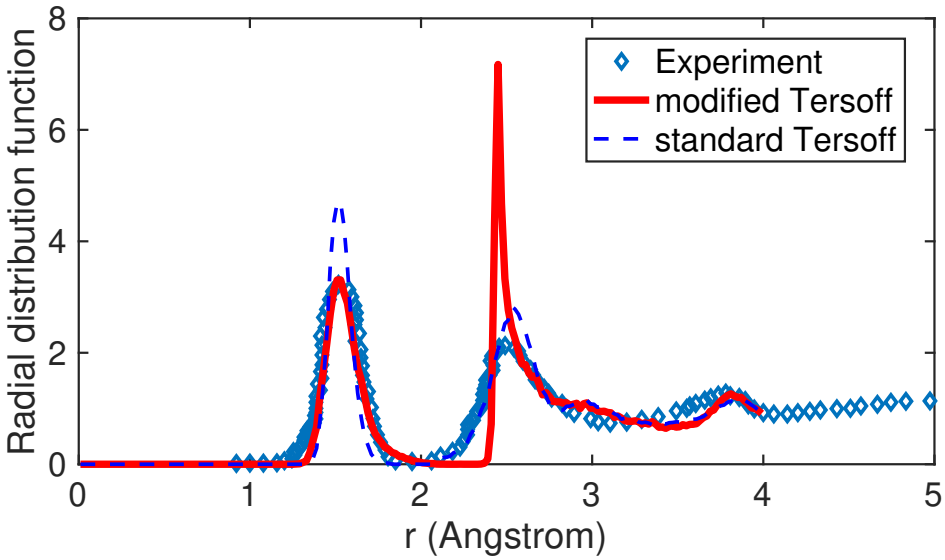

Supplementary Figure 1. Radial distribution function calculated for our amorphous carbon structures generated with the standard and modified (with extended cutoff of 2.45 Å) Tersoff potentials with a mass density of 3 g cm^{-3}. We compare the results from our simulations to experimental results (hollow diamond symbols).[1]

SUPPLEMENTARY NOTES 1: RADIAL DISTRIBUTION FUNCTION OF AMORPHOUS CARBON

Along with the correct sp^3 concentration, the model should also accurately reproduce the atomic structure of the experimentally prepared samples. Therefore, we compute the radial distribution function ($G(r)$=$4\pi[\rho(r) - \rho_0]$, where $\rho(r)$ is the atomic density at a distance r from any atom in the simulation domain and ρ_0 is the average density).[2] Figure 1 compares $G(r)$ for our structures with a mass density of 3 g cm^{-3} to experimentally determined $G(r)$ at the same mass density.[1] In general, both the modified (with extended cutoff of 2.45 Å) and the standard Tersoff potential reproduces the experimentally determined peaks reasonably well. However, the sharp peak at $\sim$2.45 Åfor the modified Tersoff potential is an artifact of the bond-order potential due to the short cutoff distance of the interatomic potential;[2–4] this is similar to the results shown by Sha et al.[2] and has also been observed for structures made with the REBO potential. We note that even though both potentials can replicate the experimental data reasonably well, the modified Tersoff potential with the relatively larger cutoff distance shows better agreement with the experimental data for r<2 Å, which is crucial in determining the sp^3 concentrations of the structures as shown

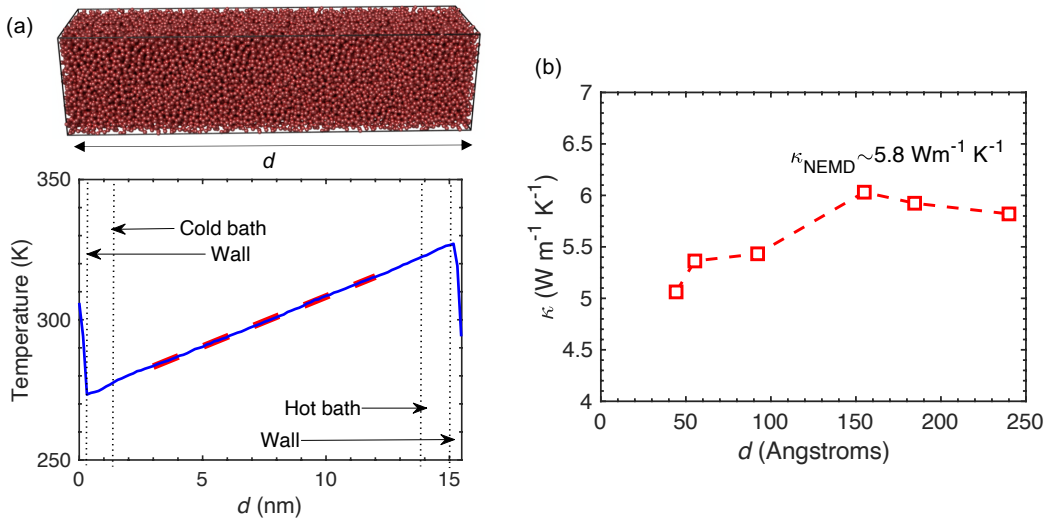

Supplementary Figure 2. (a) (Top panel) Characteristic computational domain used for our nonequilibrium molecular dynamics simulations (NEMD). We prescribe a hot and cold baths at either ends of the computational domain in the direction of the applied flux. By removing and adding equal amounts of energies from the hot and cold baths, respectively, we obtain a steady-state temperature profile from which we determine the NEMD-predicted thermal conductivities. (b) NEMD-predicted thermal conductivities as a function of domain length, d, along the heat flux applied direction. The thermal conductivities are similar for $d > 15$ nm, with an average value of $\sim$5.8 W m^{-1} K^{-1}, which agrees with our GK-predicted thermal conductivity.

in Fig. 1c of the main text.

SUPPLEMENTARY NOTES 2: NONEQUILIBRIUM MOLECULAR DYNAMICS SIMULATIONS

The calculation of atomic stress utilized in LAMMPS can result in erroneous thermal conductivities for computational domains described by some many-body interatomic potentials.[5,6] Therefore, to gain confidence in our GK-predicted thermal conductivities for our amorphous carbon domain, we run additional nonequilibrium MD (NEMD) simulations. For this purpose, we add and remove a fixed amount of energy per time step (1.6 eV fs^{-1}) to a heat bath and cold bath, respectively, that are placed at opposite ends of the computational domain. This establishes a steady-state temperature gradient across the computational domain under the microcanonical ensemble (NVE integration) where we prescribe a constant number of atoms (N), volume (V), and energy (E). We also prescribe fixed walls at either side of our computational domain as shown in

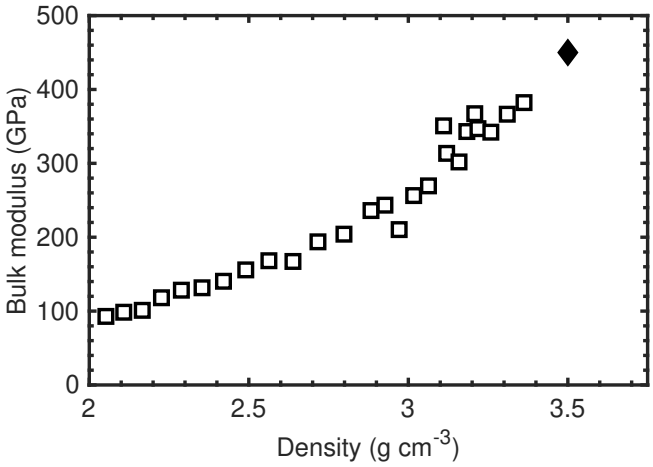

Supplementary Figure 3. Bulk modulus as a function of mass density for amorphous carbon calculated from our lattice dynamics calculations. The solid diamond symbol represents the modulus for crystalline diamond domain.

Fig. 2a. Following the evolution of a steady-state temperature profile, we average the temperature of the atoms along 100 equally spaced bins in the applied heat flux direction for a total of 10 ns as shown in Fig. 2a. Finally, we invoke Fourier's law to calculate the thermal conductivity of our simulation domains. Our fixed walls can scatter the long wavelength phonons, therefore, we calculate thermal conductivities for different domain lengths, d as shown in Fig. 2b. The NEMD-predicted thermal conductivity for our amorphous structure with a density of $\sim$3.2 g cm^{-3} is similar for $d > 15$ nm, which we prescribe as the "bulk" NEMD-predicted value.[7] This result is similar to our GK prediction for the amorphous carbon domain with a similar density (5.2 W m^{-1} K^{-1}), which provides further support for our GK-predicted thermal conductivities.

SUPPLEMENTARY NOTES 3: BULK MODULUS AND MINIMUM THERMAL CONDUCTIVITY MODEL

We calculate the bulk modulus as a function of mass density for amorphous carbon domains calculated from our lattice dynamics (LD) calculations performed with the General Utility Lattice Program (GULP) package.[8] The bulk modulus increases monotonically with density and almost reaches a similar value (for our highest density amorphous carbon domain) as that of crystalline diamond taken from Ref. 9. The increasing trend in our calculated bulk modulus is in line with the increasing Young's modulus as a function of density predicted from MD calculations utilizing the

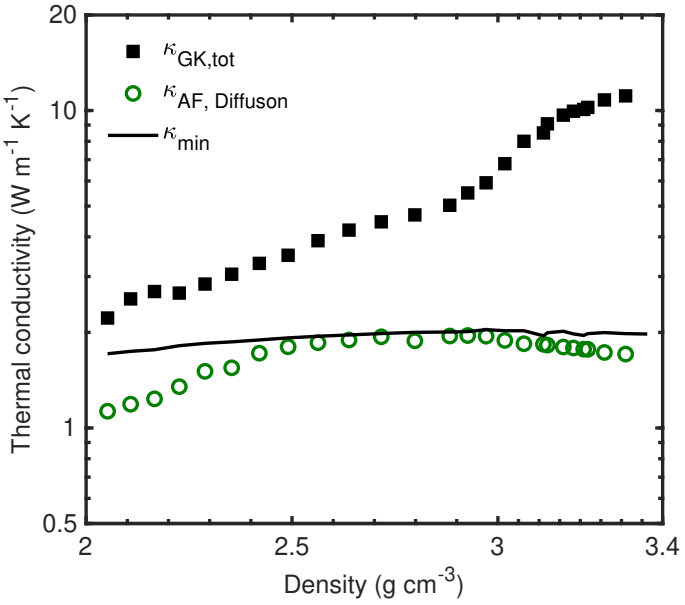

Supplementary Figure 4. Thermal conductivity as a function of mass density for our amorphous carbon domains calculated based on the minimum limit model (solid line), Green-Kubo approach and the Allen-Feldman method for diffuson thermal conductivity.

Tersoff potential.[2] We utilize the elastic constants predicted from LD calculations for our structures for the calculations of the minimum thermal conductivity model as discussed below.

The minimum thermal conductivity model as described by Cahill *et al.*[10] is given as,

$$\kappa_{\min} = \left(\frac{\pi}{6}\right)^{1/3} k_{\mathrm{B}} n^{2/3} \sum_i v_i \left(\frac{T}{\Theta_i}\right)^2 \int_0^{\Theta_i/T} \frac{x^3 e^x}{(e^x-1)^2} dx,$$

where the sum is taken over the three sound speeds (v_i), n is the atomic density, and $\Theta_i = v_i(\hbar/k_{\mathrm{B}})(6\pi^2 n)^{1/3}$ is the cutoff frequency for each polarization expressed in degrees.[10] The sound speeds for our amorphous domains are estimated based on the elastic constants calculated from our LD calculations.[11] This minimum limit model has been generally applied to pure amorphous solids where it is assumed that energy is transported through the coupling of non-propagating vibrations rather than from phonon-like propagating modes.[12] More specifically, this model assumes that the "mean free paths" of vibrations in the amorphous solid is mainly limited to the average spacing between atoms. As such, it can be expected that the model can predict the thermal conductivity calculated based on diffusons (or nonpropagating modes) dominated regime as theorized by Allen-Feldman (AF).[13]

As shown in Fig. 4, the thermal conductivities predicted by the AF model and the minimum limit model are similar for our amorphous carbon domains at different densities. However, the

minimum thermal conductivity cannot predict our Green Kubo-predicted thermal conductivities of our amorphous carbon domains since propagating (phonon-like) modes dominate heat conduction.

SUPPLEMENTARY REFERENCES

[1]F. Li and J. S. Lannin, Phys. Rev. Lett. 65, 1905 (1990).

[2]Z. Sha, P. Branicio, Q. Pei, V. Sorkin, and Y. Zhang, Computational Materials Science 67, 146 (2013).

[3]T. Kumagai, S. Hara, J. Choi, S. Izumi, and T. Kato, Journal of Applied Physics 105, 064310 (2009), https://doi.org/10.1063/1.3086631.

[4]N. A. Marks, N. C. Cooper, D. R. McKenzie, D. G. McCulloch, P. Bath, and S. P. Russo, Phys. Rev. B 65, 075411 (2002).

[5]Z. Fan, L. F. C. Pereira, H.-Q. Wang, J.-C. Zheng, D. Donadio, and A. Harju, Phys. Rev. B 92, 094301 (2015).

[6]P. Boone, H. Babaei, and C. E. Wilmer, Journal of Chemical Theory and Computation, Journal of Chemical Theory and Computation 15, 5579 (2019).

[7]D. P. Sellan, E. S. Landry, J. E. Turney, A. J. H. McGaughey, and C. H. Amon, Phys. Rev. B 81,
214305 (2010).

[8]J. D. Gale and A. L. Rohl, Molecular Simulation 29, 291 (2003).

[9]F. Aguado and V. G. Baonza, Phys. Rev. B 73, 024111 (2006).

[10]D. G. Cahill, S. K. Watson, and R. O. Pohl, Phys. Rev. B 46, 6131 (1992).

[11]A. Giri, A. Z. Chen, A. Mattoni, K. Aryana, D. Zhang, X. Hu, S.-H. Lee, J. J. Choi, and P. E. Hopkins, Nano Letters, Nano Letters 20, 3331 (2020).

[12]P. B. Allen and J. L. Feldman, Phys. Rev. Lett. 62, 645 (1989).

[13]P. B. Allen and J. L. Feldman, Phys. Rev. B 48, 12581 (1993).